J Mater Sci: Mater Electron (2015) 26:5152–5160
DOI 10.1007/s10854-015-3044-x

Aminophenoxyphthalonitrile modified MWCNTs/polyarylene ether nitriles composite films with excellent mechanical, thermal, dielectric properties

Fei Jin[1] · Mengna Feng[1] · Kun Jia[1] · Xiaobo Liu[1]

Received: 4 March 2015 / Accepted: 3 April 2015 / Published online: 17 April 2015

Abstract In this work, multi-walled carbon nanotubes (MWCNTs) were firstly surface modified with 3-aminophenoxyphthalonitrile (3-APN) via solvent-thermal method. Subsequently, modified MWCNTs were used to fabricate polyarylene ether nitrile (PEN) based composites through solution-casting technique. From the scanning electron microscope observation of 3-APN@MWCNTs/PEN composite films, 3-APN@MWCNTs had uniform dispersion and good interface compatibility with the PEN matrix. The composites were possessed and improved mechanical properties, such as the tensile strength of the composite with 4 wt% filler increased from 90 to about 110 MPa. The tensile modulus increased from 2300 to about 2750 MPa when the filler loading reached 5 wt%. Besides, the 3-APN@MWCNTs/PEN composite films exhibited excellent thermal stability, the glass transition temperature was about 228 °C and the initial decomposition temperature was beyond 484 °C. Furthermore, the dielectric constant of the composite film increased to 32.2 (50 Hz) and the corresponding dielectric loss was 0.9 with 5 wt% 3-APN@MWCNTs loading. Finally, the dynamic rheological tests were employed to investigate the molecular interaction between 3-APN@MWCNTs and PEN polymer chains.

✉ Kun Jia
jiakun@uestc.edu.cn

✉ Xiaobo Liu
liuxb@uestc.edu.cn

[1] Research Branch of Advanced Functional Materials, Institute of Microelectronic and Solid-States Electronic, High-Temperature Resistant Polymers and Composites Key Laboratory of Sichuan Province, University of Electronic Science and Technology of China, Chengdu 610054, People's Republic of China

1 Introduction

High dielectric materials with good electric energy storage have very important applications in the fields of electronics, automobile and cable industry [1–3]. With the rapid development of information, electronic and electrical industry, the polymer-based composites, possessing high dielectric constant and low dielectric loss, attract increasing research interests [4–6]. The traditional high dielectric materials mainly consist of ferroelectric ceramic materials. Although the ceramic materials have higher dielectric constant, they exhibit the disadvantages of brittleness and high processing temperature [7]. On the contrary, the polymeric materials possess good flexibility, lower processing temperature, excellent processing properties, and lower dielectric loss, but the dielectric constant is usually low with the exception of few polymers [8, 9], such as polyvinylidene fluoride, the dielectric constant is >10 (K = 12), although it is still much smaller than that of ferroelectric ceramics [10–12]. Therefore, the polymer composites, combining the advantages of inorganic nanomaterials fillers and polymer matrix, have been regarded as the good candidate for high performance dielectric materials.

MWCNTs with unique structure and excellent mechanical, electrical and chemical properties raise intensive research interests in the scientific community and industry [13–15]. Especially, MWCNTs can be used to modulate the dielectric properties of the polymer composites at very low dosage, mainly due to their special structure and high conductivity [16]. However, the pristine MWCNTs are easily agglomerated in matrix materials because of high surface energy, leading to the instability of material performance. Therefore, it is essential to ameliorate the dispersion of MWCNTs in polymer matrix. On the other hand,

polyarylene ether nitrile (PEN) exhibits excellent performances (mechanical strength, thermal stability and chemical inertia) and has been widely used as a high performance matrix for composites [17–19].

In this work, the MWCNTs were modified by amino group functionalized phthalonitrile compound (3-APN), which has potential interfacial interaction with PEN matrix, leading to the improvement of interfacial compatibility. Furthermore, the obtained 3-APN@MWCNTs was incorporated in the PEN matrix to fabricate high performance 3-APN@MWCNTs/PEN composites with enhanced dielectric, thermal and mechanical properties.

2 Experimental section

2.1 Materials

N-methylpyrrolidone (NMP, purity 99 %) and ethylene glycol was supplied by Tianjin Bodi Chemical Holding Co., Ltd., Tianjin, China. Sulfuric acid (H_2SO_4, 98 %) was provided by Shantou Xilong Chemical Factory, Guangdong, China. Nitric acid (HNO_3, 65 %) was purchased from Sichuan Xilong Chemical Co., Ltd., Sichuan, China. MWCNTs (purity 95 wt%) is about 50 nm in outer diameter, 20 μm in length, provided by Chengdu organic Chemicals Co., Ltd., Chinese Academy of Science, which was firstly purified by H_2SO_4 and HNO_3 (3:1) to remove the residual metal catalyst (Fe, etc.). PEN was provided by Union Laboratory of Special Polymers of UESTC-FEIYA, Chengdu, China. PEN (HQ/PP) was synthesized in pilot production via polycondensation of 2,6-dichlorobenzonitrile (DCBN) with phenolphthalein (PP) and hydroquinone (HQ) (molar ratio is 1:1) in the presence of anhydrous K_2CO_3 as catalyst and NMP as solvent. 3-APN was synthesized by Union Laboratory of Special Polymers of UESTC-FEIYA, Chengdu, China.

2.2 Preparation of 3-APN@MWCNTs

The 3-APN@MWCNTs was synthesized via a facile one-step solvent-thermal route. The mixture of MWCNTs, 3-APN and ethylene glycol were added into a 100 mL three necked round bottle flask with continuous ultrasonication for 2 h to achieve uniform dispersion. Then the mixture was sealed in a Teflon-lined stainless-steel autoclave, which was heated and maintained at 200 °C for 15 h. After cooling to room temperature, the composite powder was obtained by filtration and washing with ethanol and distilled water sequentially, dried in a vacuum oven at 80 °C for 12 h to obtain the 3-APN@MWCNTs. The synthesis process of 3-APN@MWCNTs was displayed in Scheme 1.

2.3 Preparation of 3-APN@MWCNTs/PEN composite films

The 3-APN@MWCNT/PEN composites were prepared by solution-casting method combined with continuous ultrasonic dispersion technology. The 3-APN@MWCNTs, PEN and NMP solvent were added into a 100 mL three necked round bottle flask equipped with a refluxing condenser and mechanical stirrer, ultrasound treating for 1 h to make sure that the 3-APN@MWCNTfillers could disperse uniformly and completely in PEN matrix. The mixture solution was cast on horizontal glass plates and dried in an oven at 80, 100, 120 and 140 °C, respectively for 1 h, followed by treatment at 160 °C for 12 h. After being cooled naturally to room temperature, the films with different 3-APN@MWCNTs loadings (0, 1, 3, 4, 5 and 6 wt%) were obtained.

2.4 Characterization

Transmission electron microscopy (TEM) was obtained on a JEOL JEM 2010 electron microscope at an accelerating voltage of 200 kV. Samples for TEM analysis were prepared by spreading a drop of dilute dispersion of the as prepared products on amorphous carbon-coated copper grids and then dried in air. Fourier transform infrared (FTIR, 200SXV, Nicolet, USA) spectra were recorded on a Perkin-Elmer Spectrum One Spectra by KBr pellet. The cross-section micromorphologies of the composite films were observed by scanning electron microscope (SEM, JEOL, JSM-5900 LV) and the samples were freeze-fractured in liquid nitrogen and then coated with a thin layer of gold before imaging. Differential scanning calorimetry (DSC) analysis was performed on a TA Instrument DSC Q100 under nitrogen atmosphere (sample purge flow 50 mL/min) at a heating rate of 10 °C/min from room temperature to 350 °C. Mechanical properties of the films were measured by employing a SANS CMT6104 Series Desktop Electromechanical Universal Testing Machine. Thermogravimetric analysis (TGA) was carried on a TA instrument Q50 series analyzer system under nitrogen atmosphere (sample purge flow 60 mL/min at a heating rate of 20 °C/min) from room temperature to 800 °C. Dielectric properties of the obtained 3-APN@MWCNTs/PEN composite films were tested by a TH 2819A precision LCR meter (Tong hui Electronic Co., Ltd.) in a frequency range from 50 Hz to 100 kHz at room temperature with 40 % humidity. Dynamic frequency sweep measurements were carried out in the angular frequency (ω) ranging from 0.01 to 100 ra s^{-1}.

Scheme 1 Synthesis process of 3-APN@MWCNTs

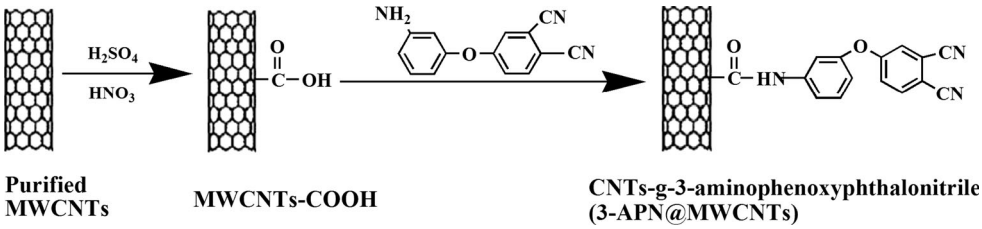

3 Results and discussions

3.1 Morphological and structure of 3-APN@MWCNTs

It is well-known that the interfacial compatibility between inorganic nanofillers and polymer matrix plays an important role in determining the overall properties of final polymer composites [20, 21]. Thus the surface morphology of pristine and amino phthalonitrile modified MWCNTs is firstly characterized by TEM. As shown in Fig. 1b, the pristine MWCNTs exhibited smooth surface morphology with the average diameter of 50 nm, while the surface of 3-APN@MWCNTs became obviously rougher (Fig. 1a), the average diameter is drastically increased to around 150 nm, indicating that the MWCNTs surface is successfully modified with phthalonitrile monomer layers. Therefore, it is assumed that the reactive polymer layers presented on the rough surface morphology of 3-APN@MWCNTs would provide numerous physical anchor sites, facilitating the subsequent molecular entanglement with polymer chains in the final composites [22, 23].

Figure 2 shows the TGA analysis and FTIR analysis of 3-APN@MWCNTs. The quantity of 3-APN that has been successfully grafted onto the MWCNTs is determined to be 6 wt% according to TGA analysis (Fig. 2a). The nature of the chemical groups on surface of MWCNTs is investigated by FTIR spectra shown in Fig. 2b. The absorption band at 3423 cm^{-1} is attributed to the hydroxyl (–OH). After modified by 3-APN, the absorption band at 1627 cm^{-1} is assigned to the C=O stretching of the amide bond (–NHCO–) [24]. Two bands at 2929 and 2859 cm^{-1} are the characteristics peaks of benzene ring. Another feature should be given attention is that the peak at 2167 cm^{-1} is characteristic peak of –CN [25]. All this observations indicated that the 3-APN has been grafted onto the MWCNTs successfully.

3.2 Morphology characterization of 3-APN@MWCNTs/PEN composite films

The fracture surface morphology of obtained 3-APN@MWCNTs/PEN film and pristine PEN film are characterized by SEM. As shown in Fig. 3a, the typical thermoplastic fracture surface morphology is observed from pristine PEN film. After adding 1 wt% of modified 3-APN@MWCNTs nanofillers into the PEN matrix, the modified MWCNTs is well-embedded in the polymer

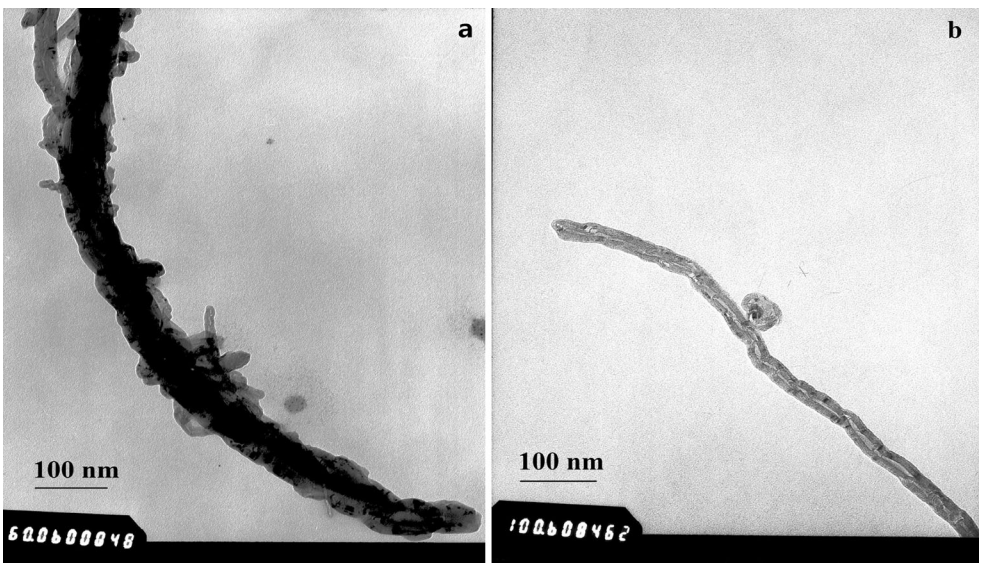

Fig. 1 TEM images of the 3-APN@MWCNTs and pristine MWCNTs

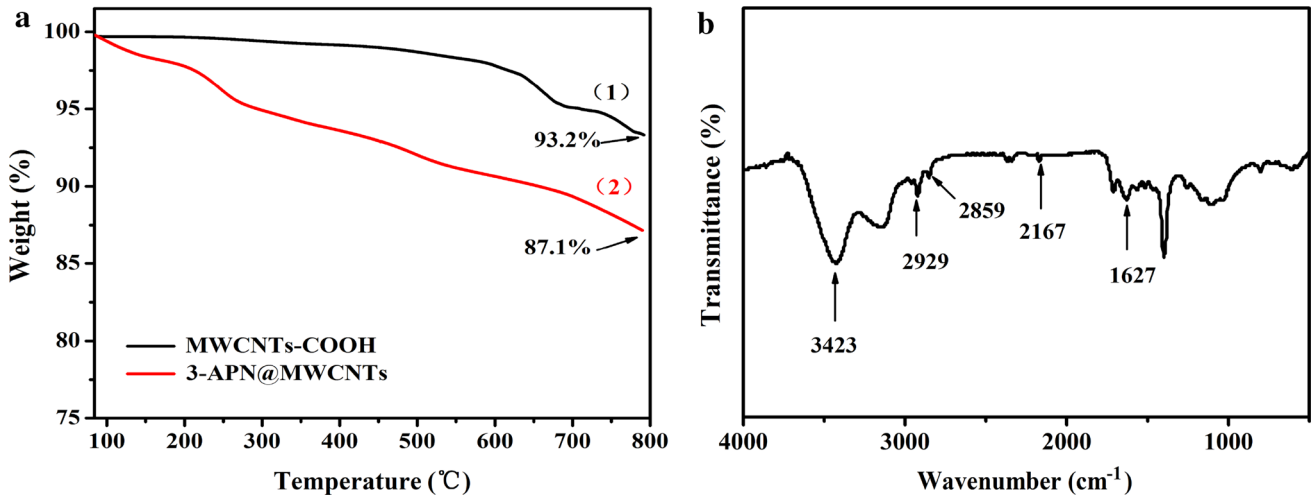

Fig. 2 **a** TGA curves of 3-APN@MWCNTs and acidified MWCNTs fillers. **b** FTIR spectra of 3-APN@MWCNTs

substrate (Fig. 3b). More importantly, no aggregation or MWCNTs bundles are captured even for a high loading content of 5 wt% 3-APN@MWCNTs (see Fig. 3c), indicating the good interfacial compatibility between 3-APN@MWCNT nanofillers and PEN matrix.

3.3 Mechanical properties of 3-APN@MWCNTs/PEN composite films

According to the previous study [23, 26], the mechanical properties of composites are dependent on the amount of fillers and the level of molecular arrangement. The high degree of aggregation as well as weak interfacial interaction also can affect tensile strength and tensile modulus of the composites. Figure 4 shows the tensile strengths and modulus of 3-APN@MWCNTs/PEN composites at varying 3-APN@MWCNTs content. It is clear that the tensile strength increased from 90 to about 110 MPa when the filler loading is 4 wt%. Besides, the tensile modulus increased from 2300 to about 2750 MPa when the filler loading reached 5 wt%. In all the tensile strength reaches their highest value at the 4 wt% 3-APN@MWCNTs loading and tensile modulus at 5 wt% 3-APN@MWCNTs loading, then a decreasing trend of strength and modulus with 3-APN@MWCNTs content occurs. The decrease of tensile strength and modulus may be caused by the fact that excessive 3-APN@MWCNTs particles cannot conglutinate entirely with PEN matrix and the physical entanglement of macromolecular chains centered on 3-APN@MWCNTs particles. However, although the slight decrease, the tensile strength and modulus of composites are still higher than that of pristine PEN except that the tensile strength with 6 wt% filler loading is slightly lower than pristine. From the above, the 3-APN@MWCNTs/PEN composites possess outstanding mechanical performances, which are attributed to the better dispersion and strong interfacial interaction between 3-APN@MWCNTs and PEN matrix. Due to the good mechanical properties, the composite films can be used in a range of practical applications.

3.4 Thermal properties of 3-APN@MWCNTs/PEN composite films

The melt behavior of pristine PEN and the 3-APN@MWCNTs/PEN composite films are analyzed by DSC and TGA. The results of thermal behavior with different 3-APN@MWCNTs contents are listed in Table 1. From the Fig. 5, we can see that the glass transition temperatures (T_g) of the composite films with different 3-APN@MWCNTs contents are all approximately 228 °C and the curves have no obvious difference, suggesting that the addition of modified inorganic filler has cannot break the stability of PEN matrix. TGA (Fig. 6) curves show that the initial decomposition temperatures (T_{id}) and the maximum decomposition rate temperatures (T_{max}) of pristine PEN are 484 and 507 °C, respectively. The T_{id} and T_{max} of the composite films are 484 ± 5 and 507 ± 4 °C, nearly independent of the loading content of 3-APN@MWCNTs. Both the DSC and TGA curves prove that the addition of 3-APN@MWCNTs almost has no effect on the thermal properties of resulted polymer composite films. Therefore, the good thermal stability of all the 3-APN@MWCNTs/PEN composites is mainly attributed to the intrinsic thermal stability of PEN matrix.

3.5 Dielectric properties of 3-APN@MWCNTs/PEN composite films

The dielectric constant and dielectric loss of the 3-APN/MWCNTs/PEN composite films are measured in the

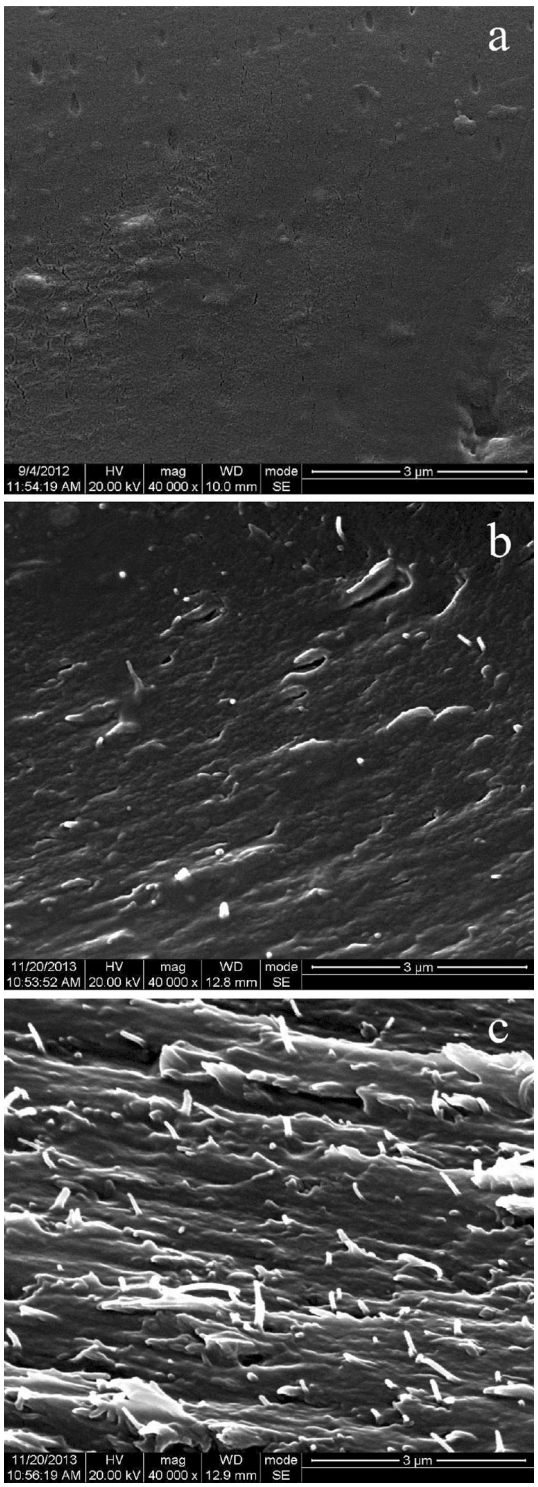

Fig. 3 Cross-section SEM images of **a** pristine PEN and the 3-APN@MWCNTs/PEN composite films with **b** 1 wt% 3-APN@MWCNTs and **c** 5 wt% 3-APN@MWCNTs loading at the magnification of 40,000

frequency range of 50 Hz–50 kHz. As shown in Fig. 7a, the dielectric constant of all the composite films decreases slightly with the increase of frequency. The decrease tendency in dielectric constant with varying frequency may be caused by the effect of polarization relaxation, specifically, there is no enough time for electric charge to polarize when the frequency field is become higher [27, 28]. The dielectric loss (Fig. 7b) exhibits the similar frequency dependence as that of dielectric constant, especially in low frequency. As can be seen, both dielectric constant and loss abruptly as the frequency increases when the loading reaches 5 wt%. It is assumed that when the 3-APN@MWCNTs content approaches a threshold value, the nanofillers tend to bridge each other and form networks. Thus it is more difficulty for the polarization rate to catch up with the frequency variation. Moreover, increased conductivity due to MWCNTs network forming is also one reason affecting the dielectric loss.

The influence of the 3-APN@MWCNTs content on the dielectric constant and dielectric loss of the films is shown in Fig. 8a, b. Obviously, the dielectric constant and dielectric loss show a linear relationship with the 3-APN@MWCNTs content when it is below 4 wt%, and there is a turning point at 4 wt%, after which the dielectric constant and dielectric loss increase abruptly with the variation of the 3-APN@MWCNTs content. It indicates that the electrical percolation threshold is about 4 wt%, after that, the curve of dielectric constant is increased slowly. The similar trend is observed for dielectric loss. According to percolation theory, $\varepsilon \infty (pc - p)^{-s}$ and $\tan\delta \infty (pc - p)^{-t}$, where Pc is theoretical percolation value, P is practical volume fraction value, s and t is critical exponent [26]. The percolation threshold theory can be used to explain this phenomenon.

3.6 Rheological behaviours of 3-APN@MWCNTs/PEN composite films

Dynamical rheological measurements are also used to investigate the rheological behaviors of the PEN composite films with various 3-APN@MWCNTs loading. The storage modulus (G') and complex viscosity (η^*) of pristine PEN and PEN composites films with different 3-APN@MWCNTs contents as a function of shear frequencies at 360 °C are plotted in Fig. 9. Figure 9a shows the effect of 3-APN@MWCNTs loading on G' of composite films, in which the magnitude of G' monotonically increases with 3-APN@MWCNTs loading, until it reached the highest value at loading 6 wt%. For the entire range of frequency, pristine PEN and PEN composite films display terminal behavior, especially at low frequency (at 0.01–0.1 rad s^{-1}). Above the high frequency, the magnitude of G' presents small tendency of slightly increase as frequency increasing, suggesting that it is not obvious affected by frequency. That is to say, the polymer molecular

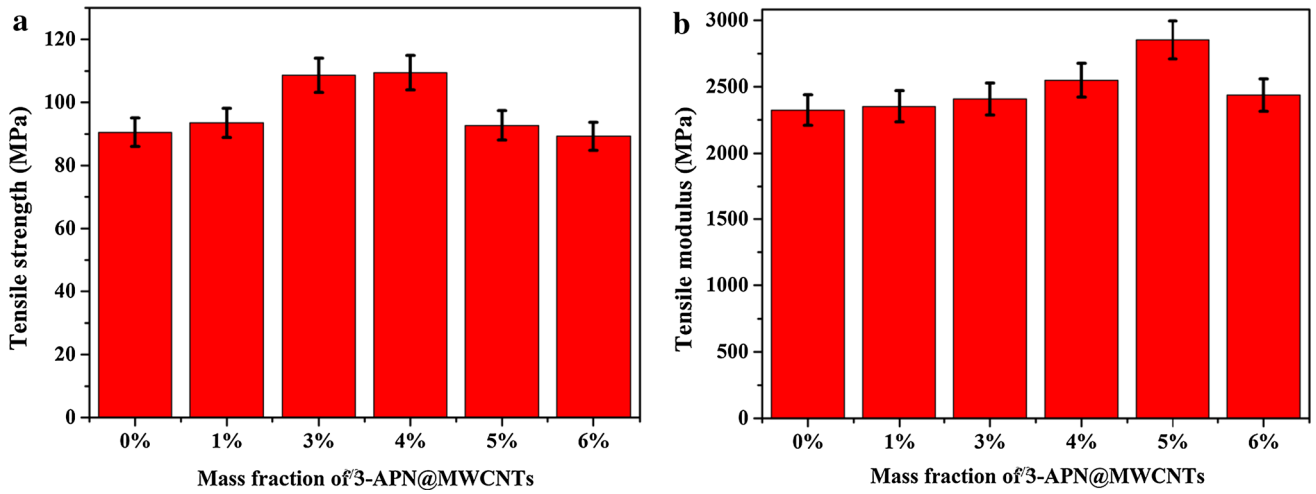

Fig. 4 **a** Tensile strength and **b** tensile modulus of pristine PEN and the 3-APN@MWCNTs/PEN composite films versus filler loading

Table 1 Thermal stabilities of pure PEN and 3-APN@MWCNTs/PEN composite films

MWCNTs content	0 wt%	1 wt%	3 wt%	4 wt%	5 wt%	6 wt%
T_g (°C)	228	228	227	226	226	228
T_{id} (°C)	484	481	487	477	479	483
T_{max} (°C)	507	505	505	503	503	503

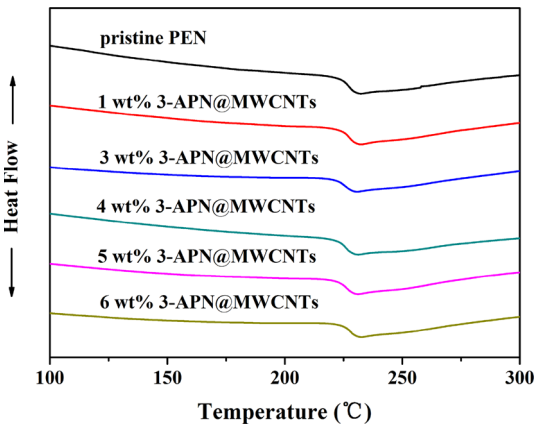

Fig. 5 DSC curves of pristine PEN and the 3-APN@MWCNTs/PEN composite films

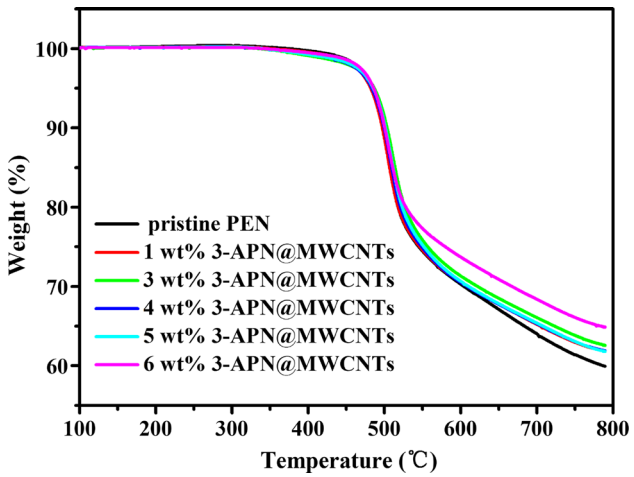

Fig. 6 TGA curves of pristine PEN and the 3-APN@MWCNTs/PEN composite films

chain motion is still controlled under in stress by frequency and the viscoelastic properties are still dominated by polymer matrix as the 3-APN@MWCNTs loading change, which maintain internal structure of liquidity. According to linear viscoelastic theory, the dynamic storage modulus (G') for homogenous polymer system is proportional to ω^2, which is consistent with Cox–Merz rule [29, 30]. Therefore, as shown in Fig. 9b, the low-frequency η^* increases with increasing of 3-APN@MWCNTs loading and finally a strong shear-thinning behavior appears. The solid-like viscoelastic response results from the formation of transient network as reported by other researchers [31], which is the characteristics of pseudoplastic fluid. Figure 10 plots the storage modulus as a function of surface modified 3-APN@MWCNTs loading at a fixed frequency (0.01 rad s^{-1}). At low loading, the filler just changes the local mobility of polymer chains. However, these restricted areas tend to interact with each other at the percolation threshold, resulting in the step change of G'. This phenomenon can be related to rheological percolation transition, at which the 3-APN@MWCNTs restrict the motion of

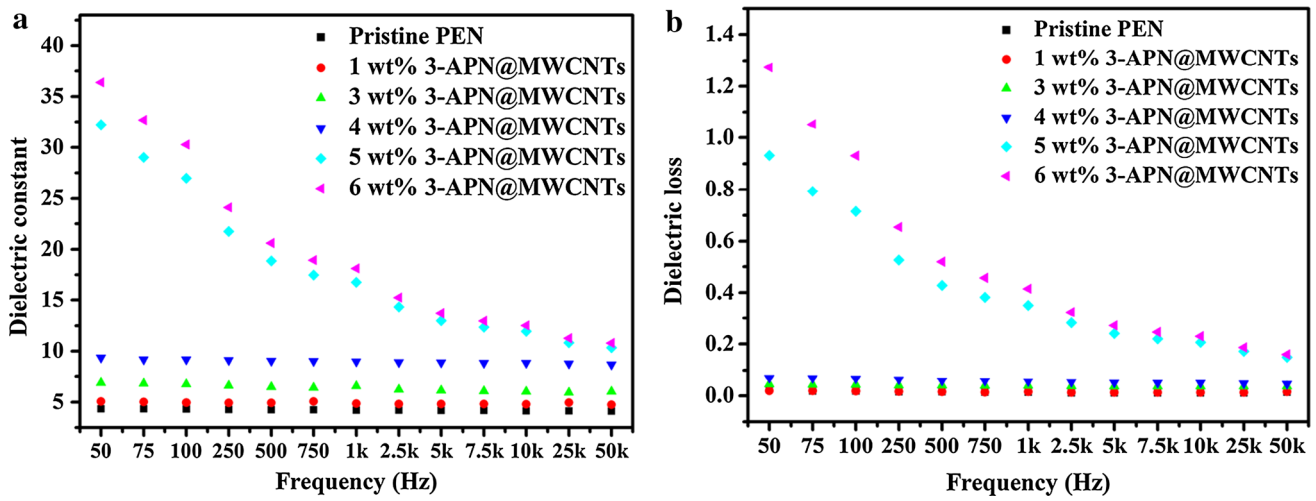

Fig. 7 **a** Dielectric constant and **b** dielectric loss of pristine PEN and the 3-APN@MWCNTs/PEN composite films as a function of frequency

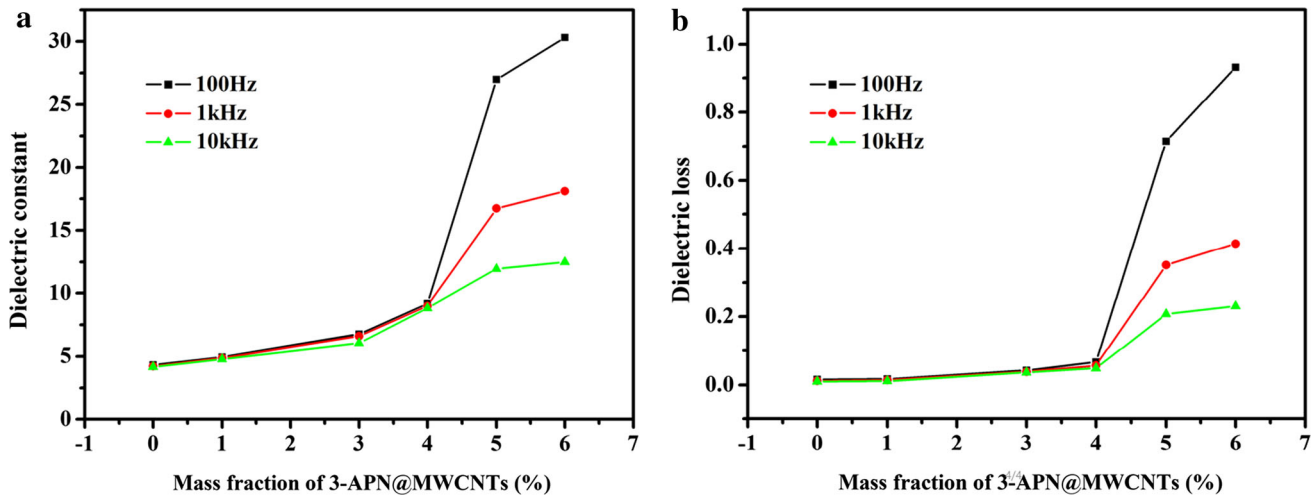

Fig. 8 **a** Dielectric constant and **b** dielectric loss of pristine PEN and the 3-APN@MWCNTs/PEN composite films as a function of filler loading at 100 Hz, 1 and 10 kHz

the polymer matrix. The calculated rheological percolation threshold is about 2.25 wt% at the fixed shear frequency (0.01 rad s^{-1}).

4 Conclusions

In summary, 3-APN@MWCNTs was synthesized via solvent-thermal route and then the polymer composite of 3-APN@MWCNTs/PEN were fabricated by solution-casting method combined with continuous ultrasonic dispersion technology. TEM, TGA and FTIR analysis showed that MWCNTs were successfully surface modified by 3-APN, avoiding the aggregation and bad dispersion with polymer matrix to a certain degree. As-prepared 3-APN@MWCNTs can be well embedded in the PEN matrix from the SEM images. Besides, the tensile strength increased from 90 to about 110 MPa when the filler loading was 4 wt%. Moreover, the tensile modulus increased from 2300 to about 2750 MPa when the filler loading reached 5 wt%. Furthermore, DSC and TGA analysis of 3-APN@MWCNTs/PEN indicated that the composite films possessed high thermal stability endowed by pristine PEN, the glass transition temperatures of the composites was all approximately 228 °C and the initial decomposition temperature is beyond 484 °C. In addition, dielectric properties of composite films were improved by adding 3-APN@MWCNTs fillers. The dielectric constant of the composite film increased to 32.2 (50 Hz), with the dielectric loss of 0.9 when the loading content of 3-APN@MWCNTs was 5 wt% and the electrical percolation threshold was around 4 wt%. Finally, the rheological characterizations showed that the composite films

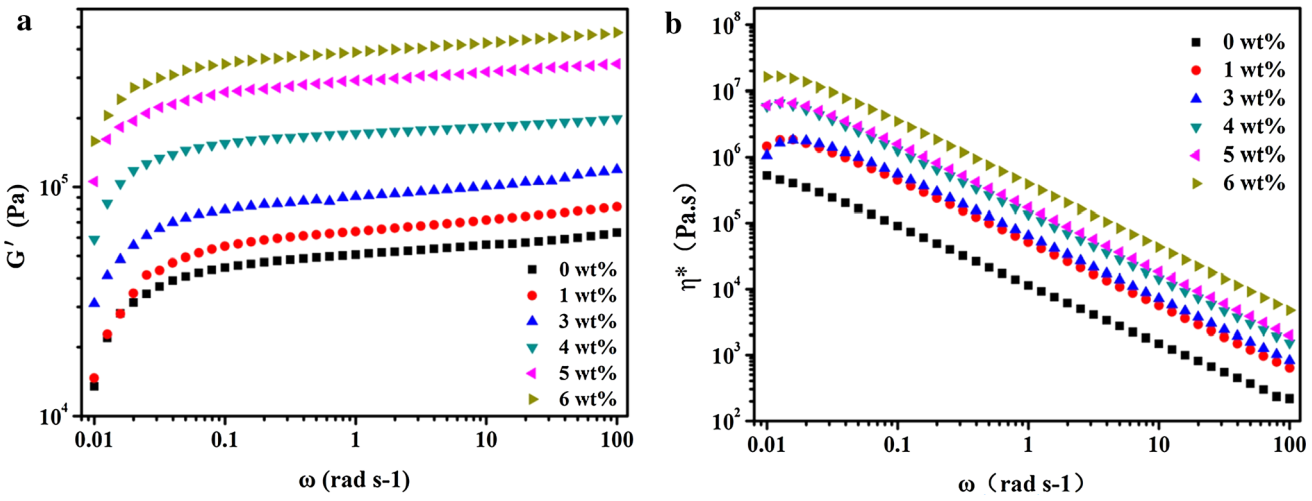

Fig. 9 **a** Dynamic storage modulus (G') and **b** complex viscosity (η^*) of the 3-APN@MWCNTs/PEN composite films obtained in dynamic frequency sweep

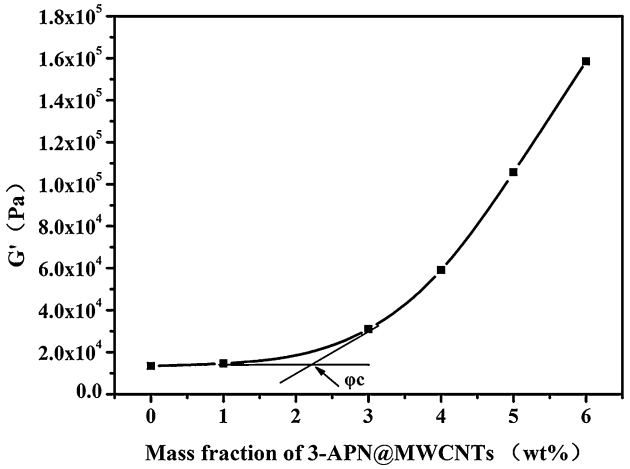

Fig. 10 Storage modulus G' of 3-APN@MWCNTs/PEN composite films as a function of filler loading at a fixed frequency of 0.01 ra s^{-1}

have a solid-like viscoelastic response at low frequencies, and the reological percolation threshold was about 2.25 wt%. Owning to excellent dispersion and strong interfacial interaction between 3-APN@MWCNTs and PEN, the fabricated composites exhibited excellent mechanical properties, good thermal stability and tunable dielectric properties, thus the 3-APN@MWCNTs/PEN composites would have potential applications in electrical engineering materials fields.

Acknowledgments The authors wish to thank for financial support of this work from the National Natural Science Foundation (Nos. 51173021, 51373028, 51403029) and "863" National Major Program of High Technology (2012AA03A212).

Conflict of interest The authors declare no conflict of interests.

References

1. M.H. Ullah, M.T. Islam, J.S. Mandeep, Int. J Appl. Electromagn. **41**, 193–198 (2013)
2. X. Yan, T. Goodson, J. Phys. Chem. B **110**, 14667–14672 (2006)
3. W. Wu, X. Huang, S. Li, P. Jiang, T. Toshikatsu, J. Phys. Chem. C **116**, 24887–24895 (2012)
4. Q. Zhang, H. Li, P. Martin, F. Xia, Z. Cheng, H. Xu, C. Huang, Nature **419**, 284–287 (2002)
5. Z. Dang, Y. Lin, C. Nan, Adv. Mater. **15**, 1625–1629 (2003)
6. L. Wang, Z. Dang, Appl. Phys. Lett. **87**, 042903 (2005)
7. M. Guo, T. Hayakawa, M. Kakimoto, T. Goodson, J. Phys. Chem. B **115**, 13419–13432 (2011)
8. Y. Rao, C. Wong, J. Appl. Polym. Sci. **92**, 2228–2230 (2004)
9. R. Ulrich, Circuit World **30**, 20–24 (2004)
10. M. Arbatti, X. Shan, Z. Cheng, Adv. Mater. **19**, 1369–1372 (2007)
11. Y. Bai, Z. Cheng, Q. Zhang, Appl. Phys. Lett. **76**, 3804–3806 (2000)
12. S. Takaya, T. Yoshinobu, K. Yasuo, F. Takeshi, M. Takeaki, Macromolecules **24**, 4691–4697 (1991)
13. B. Tang, H. Xu, Macromolecules **32**, 2569–2576 (1999)
14. S. Song, R. Rao, H. Yang, A. Zhang, J. Phys. Chem. C **114**, 13998–14003 (2010)
15. C. Chang, Y. Liu, Appl. Mater. Interfaces **3**, 2204–2208 (2011)
16. W. Liao, H. Tien, S. Hsiao, S. Li, Y. Wang, Y. Huang, S. Yang, C. Ma, Y. Wu, Appl. Mater. Interfaces **5**, 3975–3982 (2013)
17. C. Li, Y. Gu, X. Liu, Mater. Lett. **60**, 137–141 (2006)
18. A. Saxena, V. Rao, K.N. Ninan, Eur. Poly. J. **39**, 57–61 (2003)
19. H. Tang, J. Yang, J. Zhong, R. Zhao, X. Liu, Mater. Lett. **65**, 1703–1706 (2011)
20. J. Zhong, H. Tang, Y. Chen, X. Liu, J. Mater. Sci: Mater. Electron. 21, 1244–1248 (2010)
21. M. Feng, X. Huang, Z. Pu, X. Liu, J. Mater. Sci: Mater. Electron. **25**, 1393–1399 (2014)
22. X. Liu, S. Long, D. Luo, W. Chen, G. Cao, Mater. Lett. **62**, 19–22 (2008)
23. M. Feng, X. Huang, H. Tang, X. Liu, Colloids Surf. A **441**, 556–564 (2014)
24. Z. Pu, X. Huang, L. Chen, J. Yang, H. Tang, X. Liu, J. Mater. Sci: Mater. Electron. **24**, 2913–2922 (2013)

25. Y. Zhan, X. Yang, M. Feng, J. Wei, R. Zhao, X. Liu, J. Colloid Interface Sci. **363**, 98–104 (2011)
26. S. Jin, Y. Park, K.H. Yoon, Compos. Sci. Technol. **6**, 3434–3441 (2007)
27. X. Huang, Z. Pu, M. Feng, L. Tong, X. Liu, Mater. Lett. **96**, 139–142 (2013)
28. S. Xie, B. Zhu, Z. Xu, Y. Xu, Mater. Lett. **59**, 2403–2407 (2005)
29. W.P. Cox, E.H. Merz, J. Polym. Sci. **28**, 619–622 (1958)
30. Z. Pu, H. Tang, X. Huang, J. Yang, Y. Zhan, R. Zhao, X. Liu, Colloids Surf. A 415, 125–133 (2012)
31. Y. Zhan, F. Meng, X. Yang, J. Wei, J. Yang, Y. Zou, H. Guo, R. Zhao, X. Liu, J. Appl. Polym. Sci. **127**, 1827–1833 (2013)